Materials Characterization 58 (2007) 745 – 749

MATERIALS CHARACTERIZATION

# Influence of annealing on structural and optical properties of $Zn_3P_2$ thin films

R. Sathyamoorthy [a,*], C. Sharmila [a], K. Natarajan [a], S. Velumani [b]

[a] *R&D Department of Physics, Kongunadu Arts and Science College, G. N. Mills (P.O.), Coimbatore 641 029, Tamilnadu, India*
[b] *Department of Physics, ITESM-Campus, Monterrey, N.L, Mexico*

Received 30 June 2006; received in revised form 6 October 2006; accepted 16 November 2006

---

## Abstract

Zinc Phosphide films prepared by vacuum evaporation have been studied for their photovoltaic properties. X-ray diffraction studies reveal that the films are crystalline in nature and that the crystallinity improves with increase in film thickness and annealing temperature. Structural parameters such as crystallite size, strain and dislocation density are calculated for both annealed and un-annealed films and the results are discussed on the basis of film thickness and temperature. The films are highly absorbing in nature, and the transmittance and absorption seems to be thickness dependent. The band gap energy decreases with increase in film thickness as well as annealing temperature, and the possible transitions in these films are found to be direct and allowed.

*Keywords:* Zinc Phosphide; Thermal evaporation; Structural parameters; Optical band gap

---

## 1. Introduction

Zinc Phosphide was studied as early as the 1950's for its photovoltaic properties. Zinc Phosphide II–V is a polar semiconductor with mixed ionic-covalent bonds and has tetrahedral phases with $sp^3$ bonds [1]. $Zn_3P_2$ has a tetrahedral unit with atomic arrangement described by the $D_{4h}^{15}$ ($P4_2$/n mc) space group. $Zn_3P_2$ is a p-type material with a band gap of about 1.5 eV [2], it has an infrared carrier diffusion length of about 13 m [4–6], which is required to obtain a large optical absorption co-efficient ($>10^4$ $cm^{-1}$) [7]. This makes Zinc Phosphide near optimum for use in photovoltaic energy conversion. As a result, Zinc Phosphide has attracted much attention for photovoltaic applications [3]. This paper deals with the structural and optical properties of $Zn_3P_2$ films deposited under vacuum evaporation, with a comparative study between annealed and un-annealed $Zn_3P_2$ thin films.

## 2. Experimental details

Zinc Phosphide (99.999% pure, Aldrich chemicals, India) was deposited by vacuum evaporation onto well-cleaned glass substrates under a pressure of about $10^{-5}$ m bar at 303 K. A constant rate of evaporation was maintained at 5 Å/s throughout the film preparation. All the films were grown at room temperature (303 K) and a copper–constantan thermocouple was employed to measure the temperature. A rotary drive was employed to maintain uniformity in film thickness during evaporation. The thickness of the films was

---

* Corresponding author. Tel.: +91 422 2642095; fax: +91 422 2644452.
*E-mail address:* rsathya59@yahoo.co.in (R. Sathyamoorthy).

1044-5803/$ - see front matter © 2006 Elsevier Inc. All rights reserved.
doi:10.1016/j.matchar.2006.11.015

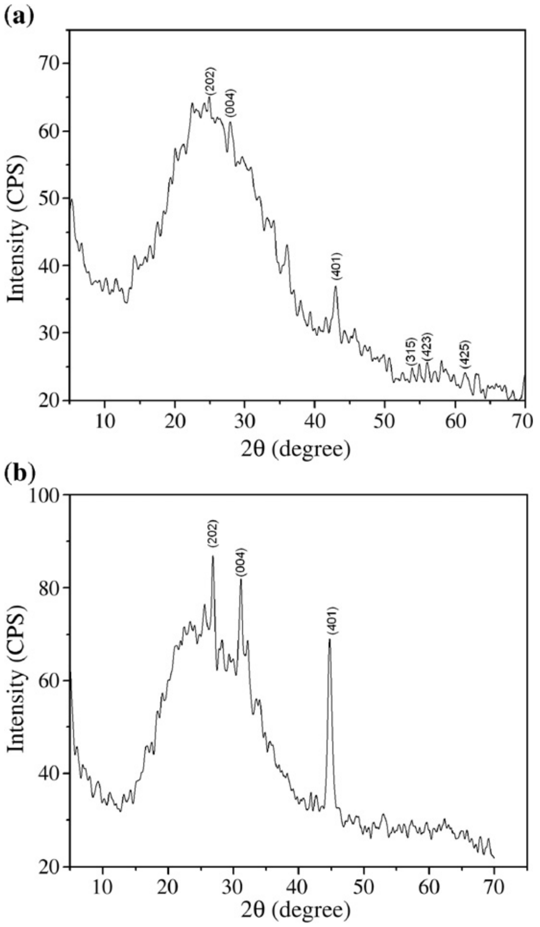

Fig. 1. XRD pattern of (a) as-grown and (b) annealed $Zn_3P_2$ film of thickness 3000 Å.

measured in-situ by a quartz crystal thickness monitor. The substrate-to-source distance was optimized to be 18 cm inside the vacuum chamber. The samples were annealed at 220 °C for 1 h in a hot air oven. The structural studies were carried out with a Shimadzu XRD-6000 X-ray diffractometer using CuKα radiation and the optical studies were carried out with a JASCO UV/VIS/NIR double beam spectrophotometer.

## 3. Results and discussion

Fig. 1a and b represents the XRD spectra of the as-deposited and annealed $Zn_3P_2$ films of thickness 3000 Å. The presence of humps for the as-deposited films leads us to understand that the $Zn_3P_2$ film has a mixed state of amorphous and microcrystalline structure. The amorphous nature arises due to the irregular arrangement of atoms and also due to the defects present in the crystal. The freshly prepared $Zn_3P_2$ films were subjected to annealing in the temperature range of 50 °C to 220 °C for 1 h in a hot air oven. It was observed that the annealed film does not show any significant change in the structure from the mixed state to a more crystalline nature until annealing above 200 °C. When $Zn_3P_2$ films are subjected to heat treatment the atoms take on a more regular arrangement, which leads to a polycrystalline nature of the film [8]. The XRD spectrum reveals that a sharp diffraction peak is observed for the diffraction angle $2\theta = 45°$ which corresponds to the (401) plane. However, a preferred orientation was also found for the diffraction angle at $2\theta = 27°$ and 30° for the (202) and (004) plane axes respectively. The observed results are in good agreement with the earlier reports [9,10]. These orientations i.e., (401), (202) and (004) are the close packed directions of the tetragonal structure and this type of ordering is often observed in polycrystalline α-$Zn_3P_2$ films [11–13]. The grain size ($D$) was calculated using the Scherrer formula [14] from the full width at half maximum (FWHM):

$$D = \frac{k\lambda}{\beta \cos\theta} \tag{1}$$

where, the constant $k$ is the shape factor ≈0.94, $\lambda$ is the wavelength of the X-rays (1.5406 Å for CuKα), $\theta$ is the Bragg's angle and $\beta$ is the FWHM. The

Table 1
Structural parameters of as-grown $Zn_3P_2$ films

| Thickness | Experimental | | Theoretical | | FWHM | Grain size $D$ | Strain (ε) | Dislocation density |
|---|---|---|---|---|---|---|---|---|
| Å | $2\theta$ | $d$ (Å) | $d$ (Å) | $h\ k\ l$ | Degree | nm | $\text{lin}^{-2}\ \text{m}^{-4}$ | $10^{14}$ lines/m$^2$ |
| 3000 | 44.38 | 2.039 | 2.010 | 4 0 1 | 0.2400 | 34.6 | 10.46 | 8.35 |
| 5000 | 45.07 | 2.010 | 2.010 | 4 0 1 | 0.0900 | 92.24 | 3.92 | 1.175 |
| 10,000 | 45.02 | 2.012 | 2.010 | 4 0 1 | 0.0800 | 103.80 | 3.48 | 0.928 |
| 18,000 | 45.12 | 2.007 | 2.010 | 4 0 1 | 0.0400 | 207.59 | 1.74 | 0.232 |

Table 2
Structural parameters of annealed $Zn_3P_2$ films

| Thickness | Experimental | | Theoretical | | FWHM | Grain size *D* | Strain (ε) | Dislocation density |
|---|---|---|---|---|---|---|---|---|
| Å | 2*θ* | *d* (Å) | *d* (Å) | *h k l* | Degree | nm | $lin^{-2}\ m^{-4}$ | $10^{14}$ lines/$m^2$ |
| 3000 | 44.20 | 2.024 | 2.010 | 4 0 1 | 0.5200 | 15.36 | 22.67 | 42.38 |
| 5000 | 45.14 | 2.050 | 2.010 | 4 0 1 | 0.0400 | 207.58 | 1.74 | 0.232 |
| 10,000 | 45.97 | 2.014 | 2.010 | 4 0 1 | 0.1400 | 59.31 | 6.10 | 2.842 |
| 18,000 | 45.27 | 2.001 | 2.010 | 4 0 1 | 0.1467 | 56.60 | 6.39 | 3.125 |

dislocation density (δ) can be evaluated from the crystallite size (*D*) by the following relation:

$$\delta = \frac{1}{D^2} \qquad (2)$$

The micro strain (ε) can be calculated from the following relation:

$$\varepsilon = \frac{\beta\cos\theta}{4}. \qquad (3)$$

The structural parameters were calculated and the results are given in Tables 1 and 2 for as-deposited and annealed $Zn_3P_2$ films of different thickness. For as-deposited films it is seen that the grain size (*D*) increases with an increase in film thickness. This may be due to columnar grain growth [15]. For annealed films it is observed that the grain size increases as thickness increases from 3000 to 5000 Å, whereas there is a decrease in grain size with thickness increasing from 5000 to 18,000 Å. This grain size increase may be due to the columnar growth, while the decrease in grain size may be due to the formation of secondary grains on the film surface [16]. The strain ε of the films decreases with an increase in film thickness for as-deposited films, while the annealed films show an increase in strain, which may be due to thermal strain. The dislocation density δ decreases for annealed films when compared to as-deposited films, and this is due to atomic motion under heat treatment, which causes a decrease in dislocation density [17].

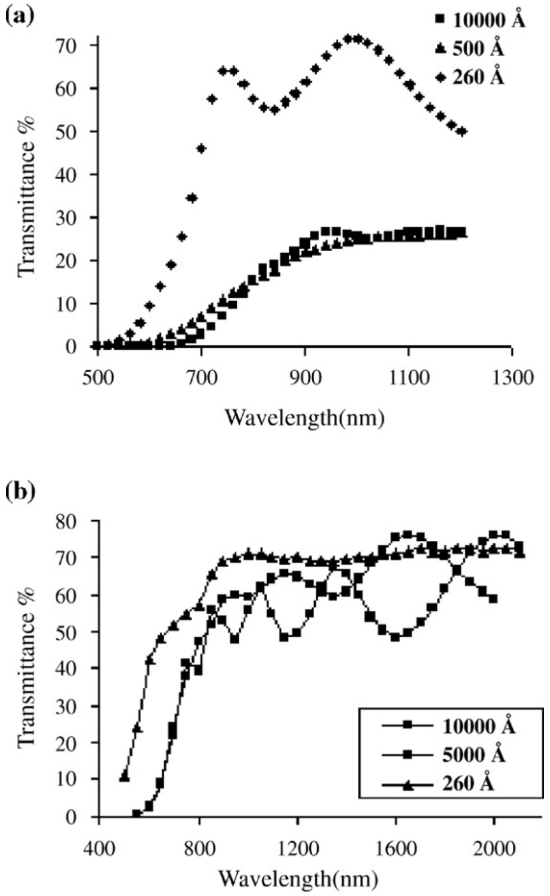

Fig. 2. Transmission spectra of (a) as-grown and (b) annealed $Zn_3P_2$ films.

## 4. Optical properties

The transmission spectra for as-deposited and annealed films are shown in Fig. 2a and b. It is found that the percentage of transmittance decreases with increase in film thickness. For annealed samples the transmittance spectra exhibit good maxima and minima when compared to the as-deposited samples [18]. This

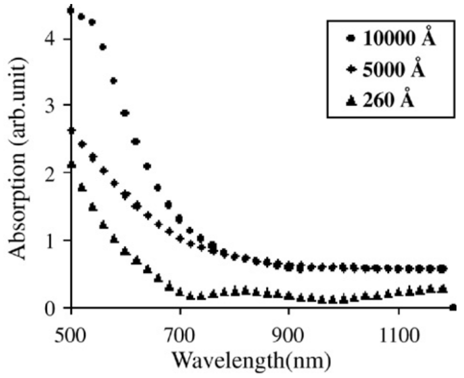

Fig. 3. Absorption spectra of as-grown Zinc Phosphide films of different thicknesses.

indicates improvement of internal film morphology and uniformity upon annealing. The absorption spectra measured as a function of photon wavelength for as-deposited films of thickness 260, 5000 and 10,000 Å is shown in Fig. 3. From the graph it can be positively concluded that the films are highly absorbing in nature, which is suitable for photovoltaic applications [19].

The energy dependence of the absorption coefficient α near the band edge for band-to-band and exciton transitions in terms of the incident radiation energy are given below:

$$\alpha = A(hv - E_g)^P \tag{4}$$

where, '$A$' is a constant, '$E_g$' is the energy band gap, '$v$' is the frequency of the incident radiation and '$h$' is Plank's constant. The magnitude of the exponent $P$ is characteristic of the type of transition, and takes the value 1/2, 3/2, 2 and 3 for direct, allowed forbidden, indirect allowed and indirect forbidden transitions respectively. $Zn_3P_2$ is a direct gap material and plotting $(\alpha hv)^2$ against the photon energy ($hv$) (Fig. 4a and b) can give the band gap energy by extrapolating the linear portion to the energy axis.

**(a) 5000 Å as-grown**

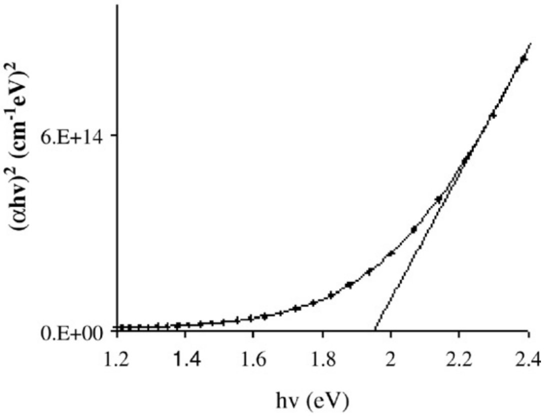

**(b) 5000 Å annealed**

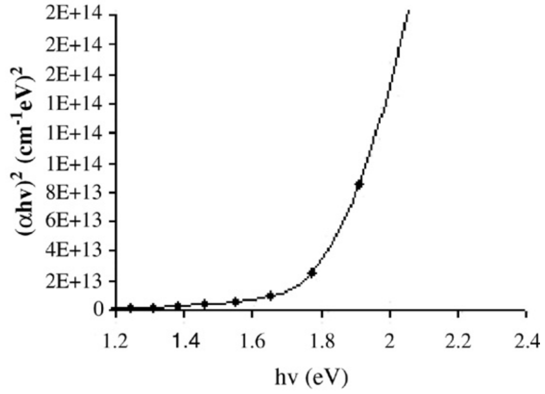

Fig. 4. $(\alpha hv)^2$ versus photon energy for $Zn_3P_2$ films.

Table 3
Band gap energy for $Zn_3P_2$ films of different thicknesses

| Thickness (Å) | Band gap energy of as grown $Zn_3P_2$ films (eV) | Band gap energy of annealed $Zn_3P_2$ films (eV) |
|---|---|---|
| 260 | 2.20 | 2.00 |
| 5000 | 1.90 | 1.78 |
| 10,000 | 1.70 | 1.68 |
| 18,000 | 1.40 | 1.39 |

The band gap energy was estimated from the plots and is given in the Table 3 for as-deposited and annealed Zinc Phosphide films. From Table 3 it is seen that the band gap energy decreases with the increase in film thickness. The estimated band gap values are in good agreement with the earlier reports [20]. This decrease in optical band gap energy may be due to many reasons, including the presence of an internal electric field associated with the defects in the film, or the increased grain growth of the film at higher thickness.

## 5. Conclusions

The structure of $Zn_3P_2$ films was found to be amorphous and polycrystalline for films of lower and higher thickness respectively. The grain size increases with the increase in film thickness for as-grown films whereas the strain and dislocation density decreases. The grain size decreases due to annealing as a result of a quantum size effect. The material is of a highly absorbing nature. The band gap energy decreases with the increase in film thickness and annealing temperature. The optical transition is found to be direct and allowed.

## Acknowledgements

The authors wish to acknowledge the Secretary and the management of Kongunadu Arts and Science College, Coimbatore for their encouragement and support to carryout this work. One of the authors (RS) gratefully acknowledges University Grants Commission (UGC), New Delhi for awarding UGC-Research Award-Project No. F-30-1/2004 (SA-II).

## References

[1] Suchet J. Chemical physics of semiconductors. London: Van Nostrand Co, Ltd.; 1967.
[2] Sberveglieri G, Romeo N. Quasi-rheotaxial growth of $Zn_3P_2$. Thin Solid Films 1981;83:L133–6.

[3] Catalona Dalal V, Fagen EA, Hall RB, Masi JV, Meakin LD, Warfield G, et al. Proc Intern Photovoltaic solar energy conf, Luxembourg; 1977.

[4] Weber A, Sutter P, Von Kanel H. Amorphous $Zn_3P_2$ thin films grown by reactive R.F. sputtering. Thin Solid Films 1994;239:205–10.

[5] Convers Wyeth N, Catalano A. Spectral response measurements of minority-carrier diffusion length in $Zn_3P_2$. J Appl Phys 1979;50:1403–7.

[6] Kakishita Kazuhiko, Ikeda Shusaku, Suda Toshikazu. $Zn_3P_2$ epitaxial growth by MOCVD. J Cryst Growth 1991;115:793–7.

[7] Suda Toshikazu, Miyakawa Tadashi, Kurita Shoichi. Zinc Phosphide thin films grown by RF sputtering. J Cryst Growth 1988;86:423–35.

[8] Imai T, Fuke Shunro, Kawarabayashi Shigeru, Kuwahara Kazuhiro. X-ray diffraction studies on polycrystalline $Zn_3P_2$ films deposited by hot wall method. Appl Surf Sci 1988;33/34: 594–601.

[9] Weber A, Sutter P, Von Kanel H. Growth of amorphous Zinc Phosphide films by reactive radio frequency sputtering. J Non-Cryst Solids 1993;164:79–82.

[10] Weber A, Sutter P, Von Kanel H. Optical, electrical and photoelectrical properties of sputtered thin amorphous $Zn_3P_2$ films. J Appl Phys 1994;75:7448–55.

[11] Chu TL, Shirley Chu S, Murthy K, Stokes ED, Russell PE. J Appl Phys 1983;54:2063–8.

[12] Lousa A, Bertran E, Varela M, Moreenza JL. Deposition of $Zn_3P_2$ thin films by coevaporation. Sol Energy Mater 1985;12:51–6.

[13] ASTM X-ray powder data file, sets 1–5, Inorganic volume PDIS 5iRB, File no 2-1264 (1960).

[14] Cullity BD. Elements of X-ray diffraction. Massachuselts: Additional-Wesley Publishing Company; 1967.

[15] Fuke Shunro, Imai Tetsuji, Kawasaki Kazushige, Kuwahara Kazuhiro. Substrate effect on the deposition of $Zn_3P_2$ thin films prepared by a hot-wall method. J Appl Phys 1989;65:564–6.

[16] Kakishita Kazuhiko, Baba Toshio, Suda Toshikazu. $Zn_3P_2$ thin films grown on glass substrates by MOCVD. Thin Solid films 1998;334:25–9.

[17] Dheepa J, Sathyamoorthy R, Velumani S, Subbarayan A, Natarajan K, Sebastian PJ. Electrical resistivity of thermally evaporated bismuth telluride thin films. Sol Energy Mater Sol Cells 2004;81:305–12.

[18] Aranda J, Morenza JL, Esteve J, Codina JM. Optical properties of vacuum-evaporated CdTe thin films. Thin Solid Films 1984;120:23–30.

[19] Bryja L, Jezierski K, Ciorga M, Bohdziewicz A, Misiewicz J. Temperature dependence of energy gap of amorphous thin films of $Zn_3P_2$. Vacuum 1998;50:5–7.

[20] Hermann AM, Madan Arun, Wanlass MW, Badri V, Ahrenkiel R, Morrison Scott, et al. MOCVD growth and properties of $Zn_3P_2$ and $Cd_3P_2$ films for thermal photovoltaic applications. Sol Energy Mater Sol Cells 2004;82:241.